



Heat-induced endoplasmic reticulum stress in soleus and gastrocnemius muscles and differential response to UPR pathway in rats

Shivani Sharma^{1,2} · Pooja Chaudhary¹ · Rajat Sandhir² · Abhishek Bharadwaj¹ · Rajinder K. Gupta¹ · Rahul Khatri¹ · Amir Chand Bajaj¹ · T. P. Baburaj¹ · Sachin Kumar¹ · M. S. Pal¹ · Prasanna K. Reddy¹ · Bhuvnesh Kumar¹

Received: 8 May 2020 / Revised: 29 October 2020 / Accepted: 3 November 2020 / Published online: 18 November 2020
© Cell Stress Society International 2020

Abstract

The present study aimed to investigate the differential response of oxidative (soleus) and glycolytic (gastrocnemius) muscles to heat-induced endoplasmic reticulum (ER) stress. It was hypothesized that due to compositional and functional differences, both muscles respond differently to acute heat stress. To address this, male Sprague Dawley rats (12/group) were subjected to thermoneutral (25 °C) or heat stress (42 °C) conditions for 1 h. Soleus and gastrocnemius muscles were removed for analysis post-exposure. A significant increase in body temperature and free radical generation was observed in both the muscles following heat exposure. This further caused a significant increase in protein carbonyl content, AOPP, and lipid peroxidation in heat-stressed muscles. These changes were more pronounced in heat-stressed soleus compared to the gastrocnemius muscle. Accumulation of unfolded, denatured proteins results in ER stress, causing activation of unfolded protein response (UPR) pathway. The expressions of UPR transducers were significantly higher in soleus as compared to the gastrocnemius muscle. A significant elevation in resting intracellular calcium ion was also observed in heat-stressed soleus muscle. Overloading of cells with misfolded proteins in soleus muscle activated ER-induced apoptosis as indicated by significant upregulation of C/EBP homologous protein and Caspase12. The study provides a detailed mechanistic representation of the differential response of muscles toward UPR under heat stress. Data suggests that soleus majorly being an oxidative muscle is more prone to heat stress-induced insult indicated by enhanced apoptosis. This study may aid in devising mitigation strategies to improve muscle performance under heat stress.

Keywords Heat stress · Unfolded protein response · Soleus muscle · Gastrocnemius muscle · Oxidative stress · Apoptosis

Abbreviations

HS	Heat stress
GS	Gastrocnemius
SL	Soleus
ER	Endoplasmic reticulum
UPR	Unfolded protein response

Introduction

Every homeothermic organism operates at a fixed temperature range known as the thermoneutral zone at which they can maintain an adequate balance between heat production and loss thereby attaining homeostasis (Swanlund et al. 2008). Exposure to high environmental temperature and strenuous physical activities can cause excessive gain in thermal energy exceeding the thermoneutral zone leading to heat stress. Heat stress has been shown to increase core as well as tissue temperature, depress immunity, lead to electrolyte imbalance, impair endocrine and reproductive functions, increase cortisol and corticosterone levels, and cause early onset of fatigue (Lin et al. 2006; Allen 2009; Yahav 2009; Syafwan et al. 2011; Renaudeau et al. 2012; Lara and Rostagno 2013; Loyau et al. 2014). Heat stress causes numerous alterations at the cellular level as well such as an increase in the fluidity of

✉ Pooja Chaudhary
poojachaudhary155@gmail.com

¹ Defence Institute of Physiology and Allied Sciences (DIPAS), DRDO, Timarpur, Delhi 110054, India

² Department of Biochemistry, Panjab University, sector 25, Chandigarh, India

membrane lipids, loss of membrane integrity, and inactivation of enzymes in mitochondria thereby disrupting cellular homeostasis (Sawka et al. 2011; Richter et al. 2010; Roti Roti 2008; Hildebrandt et al. 2002; Sonna et al. 2002; Lindquist 1986; Lima et al. 2013). The major effect of heat stress is protein denaturation and aggregation (Lepock and Borrelli 2005), resulting in cell cycle arrest, inactivation of protein synthesis, and inhibition of deoxyribonucleic acid (DNA) repair. Heat stress exerts considerable effects on the physiological functions and physical performance of an individual (Tattersson et al. 2000).

Heat stress has been shown to negatively impact muscle growth (Close and Mount 1971; Versteegen et al. 1973) and is acknowledged as an inducer of oxidative stress in skeletal muscle (Mujahid et al. 2005; Altan et al. 2003; Sahin et al. 2003). Increased free radical generation due to heat stress leads to disruption of redox balance (Azad et al. 2010; Kikusato and Toyomizu 2013). Furthermore, some studies have revealed that oxidative stress can cause protein degradation through enhanced proteolysis and autophagy (McClung et al. 2009, 2010; Dodd et al. 2010; Whidden et al. 2010; Smuder et al. 2012). Oxidative stress also impairs protein synthesis by inhibiting translation (Shenton et al. 2006; Zhang et al. 2009). The balance between new protein synthesis and degradation is essential to maintain a steady state level of proteins in the body. However, oxidative stress decreases the overall protein turnover rate in skeletal muscles. Skeletal muscle is a highly dynamic and plastic tissue, comprising approximately 40% of total body mass and 50–75% of all body proteins (Frontera and Ochala 2015). They are responsible for a plethora of functions including posture, endurance, and ballistic movements (Lindstedt et al. 2013). During strenuous physical activities, the blood flow is increased in the muscles. The largest of these increases occurs in the exercising skeletal muscles. Therefore, during maximal exertion, skeletal muscles act as sink and consume nearly all the oxygen inhaled by the individual in order to sustain enhanced energy demands (Lindstedt 2016). However, adverse alterations occurring in skeletal muscles negatively impact physical performance under stressful conditions such as hot humid environments.

Skeletal muscles possess an extensive network of specialized endoplasmic reticulum (ER) called sarcoplasmic reticulum. The endoplasmic reticulum (ER) is a vital membrane-bound organelle responsible for the synthesis, initial post-translational modification, proper folding, maturation of newly synthesized transmembrane, and secretory proteins. ER also serves as a dynamic pool of calcium, regulating the intracellular calcium homeostasis. Additionally, it is a critical site for lipid biosynthesis, detoxification, energy metabolism, and maintenance of redox balance in skeletal muscle (Deldicque 2013). Various physiological and pathological circumstances such as accumulation of unfolded proteins, oxidative stress,

disruption of calcium homeostasis, metabolic challenges, and viral infection as well as an alteration in redox status can compromise protein folding in ER (Wang and Kaufman 2016). Particularly, protein folding and disulfide bond formation in the ER lumen are highly sensitive to redox state. Oxidative stress can disrupt the protein folding mechanism and enhance the accumulation of unfolded proteins causing ER stress (Malhotra and Kaufman 2007). Also, alterations in the ER-regulated protein folding pathway results in the excessive free radical generation and exacerbate oxidative stress. A growing number of studies support the view that ER stress and oxidative stress regulate each other in a positive feed-forward loop, which intervenes in normal cellular functions and activates pro-apoptotic pathways (Cao and Kaufman 2014).

To resolve ER stress, cells use an adaptive mechanism known as unfolded protein response (UPR). UPR is a series of events or signaling pathway that serves to restore ER functions by inducing chaperone production, diminishing protein translation, and removing accumulated misfolded proteins (Wu and Kaufman 2006; Chakrabarti et al. 2011). The UPR is controlled by three ER-transmembrane stress sensors, namely inositol-requiring enzyme 1 α (IRE1 α), pancreatic endoplasmic reticulum kinase (PERK), and activating transcription factor 6 (ATF6). Under physiological conditions, these sensors remain bound to ER-resident chaperone BIP/GRP78 (78-kDa glucose-regulated protein) through their luminal domain and kept in an inactive state. Upon accumulation of unfolded/misfolded proteins, each transducer can disassociate from Bip and becomes activated (Gething 1999). Release of Bip results in oligomerization and activation of the two kinases PERK and IRE1 α which engages in an intricate downstream signaling pathway. Upon activation, PERK induces eukaryotic initiation factor 2 alpha subunit (eIF2 α) kinase and phosphorylation of eIF2 α resulting in attenuation of protein synthesis (Harding et al. 1999). Activation of IRE1 α leads to the induction of genes responsible for regulating protein quality control in the ER (Xu et al. 2005). Translocation of ATF6 to the Golgi apparatus leads to its cleavage to form an active transcription factor, activating the third branch of UPR. This factor then migrates to the nucleus and mediates activation of UPR-targeted genes such as chaperones (Adams et al. 2019).

Although ER stress is usually a short-term event, resolved by UPR activation, but prolonged and severe ER stress triggers apoptosis (Ron and Walter 2007; Zhang and Kaufman 2008). Apoptosis is initiated through two major pathways, the cell-intrinsic, mitochondrial pathway regulated by the Bcl2 protein family, and cell-extrinsic, death receptor pathway (Danial and Korsmeyer 2004). Both the pathways ultimately converge to activate caspase cascades. There remains considerable debate about how UPR signaling engages with these core apoptotic pathways. A prominent role of C/EBP homologous protein (CHOP) and caspase12 has been proposed in

ER stress-induced cell death, which ultimately engages with the core apoptotic pathways and activates caspase cascade (Nakagawa et al. 2000; Kaufman 2002; Logue et al. 2013).

Although skeletal muscle contains an extensive network of ER, the role of ER stress and UPR in the regulation of skeletal muscle pathology under heat stress remains understudied. The purpose of this study was to determine the extent to which acute heat exposure induces changes in ER stress response in soleus (SL) and gastrocnemius (GS) muscle. SL and GS are the muscles of hindlimbs and form the calf. GS is the larger muscle forming the bulge in the calf while SL is a smaller flat muscle lying underneath the GS muscle. Both the muscles vary in their composition as well as in function. SL is an oxidative muscle while GS is majorly a glycolytic muscle. The study aimed at examining the effects of acute heat exposure on individual arms of the UPR pathway and how differently these two muscles respond to the same amount of stress. The present study hypothesizes that due to compositional differences, both muscles vary in their response toward acute heat exposure, and SL being an oxidative muscle is more susceptible to heat-induced injuries. This study provides detailed insight into the differential response of oxidative and glycolytic muscles and may help in devising strategies to improve muscle performance under heat stress.

Materials and methods

Ethics statement

All experiments and procedures were approved by the Animal Ethical Committee of the Institute (IAEC/DIPAS/2017-18) as per Committee for the Purpose of Control and Supervision of Experiments on Animals (CPCSEA) of the Government of India. The care of all study animals was in accordance with the institutional animal care and use committee (IACUC).

Animals and experimental design

The study was conducted on twenty-four male Sprague Dawley rats 6–8 weeks old, physiologically fit and sexually mature averaging weighing 230 ± 20 g, maintained in an animal facility of the Defence Institute of Physiology and Allied Sciences (DIPAS). Rats were housed three animals per cage at 25 ± 1 °C, $55 \pm 10\%$ relative humidity (RH), and given ad libitum food (5 g/100 g body weight/day) and water (average consumption 10 ml/100 g body weight/day) under 12-h light and dark cycle. After a week of acclimatization, rats were randomly divided into two groups of twelve rats each.

Group 1: Control (C), exposed to 25 ± 1 °C, $40 \pm 10\%$ RH for 1 h

Group 2: Heat stress (HS), exposed to 42 ± 1 °C, $40 \pm 10\%$ RH for 1 h

Rats from both the groups were exposed to the respective temperatures in a simulation chamber (Animal climatic chamber, Macroscientific (MAC), India) during the daytime for 1 h. The climatic chamber for animal exposures is forced convection type and was custom made with a glass double door system. It has a temperature and humidity controller and a digital display to observe the set and process values for temperature and humidity. It comes with air ducts guarded by HEPA filters for air purification. During the exposure, the animals were given no access to food and water. The weight of animals was recorded after the exposure. Animals exposed to 42 °C showed a non-significant reduction in weight (data not shown). After the completion of exposures, the rats were dissected for soleus (SL) and gastrocnemius (GS) muscles and kept at -80 °C for further experiments.

Core, skin, and muscle temperature

The core and skin temperatures of rats were monitored during the exposure using a thermistor and t-type pods for LabChart 8.1.3 (ADInstruments). The core temperature of animals was measured by inserting the rectal probe 1 cm inside the rectum (thermistor (RET-2) MLT1403, AD Instruments). The reading was obtained 10 s after insertion into the rectum. The skin temperature was measured using a skin temperature probe ((2 m), MLT422/A, AD Instruments) by neatly placing it on the upper part of the tail and covering it with adhesive tape. Muscle temperature was recorded immediately after the exposures using micro YSI probes (YSI 521, YSI, Yellow Springs Instruments, USA) (Dollberg et al. 1993). The muscles were exposed by incising the skin, and using these probes, the temperature of both SL and GS muscles was recorded.

Oxidative stress markers

Free radical generation Free radical generation was measured fluorimetrically using 2,7-dichlorofluorescein diacetate (DCFH-DA) (Agrawal et al. 2017). DCFH-DA permeabilizes the cell and gets hydrolyzed intracellularly by esterases to form DCFH carboxylate anion. DCFH is further oxidized by free radicals to form a highly fluorescent product, dichlorofluorescein (DCF), emitting fluorescence in the presence of free radicals. In this method, 150 μ l of tissue homogenate homogenized in 0.154 M KCl-EDTA buffer was incubated with 10 μ l of 100 μ M DCFH-DA for 30 min in dark at room temperature (RT). Fluorescence was then read using a fluorimeter (TECAN, Infinite 200pro) with excitation at 485 nm and emission at 535 nm. Readings were obtained in arbitrary fluorometric units (AFU).

Lipid peroxidation Malondialdehyde (MDA), a lipid peroxidation product, was measured in muscle homogenate using the method of Buege and Aust (1978). The detection of MDA is based on the reaction with thiobarbituric acid (TBA) in acidic pH at 90–100 °C. Proteins in the homogenate are precipitated with trichloroacetic acid (TCA) followed by a reaction with TBA resulting in the formation of a pink colored pigment, which is measured spectrophotometrically. In this method, 10% tissue homogenate was prepared in TBA:TCA (1:1) buffer, which was then subjected to boiling for 30 min. Then, the homogenate was centrifuged at 1200g for 10 min and supernatant was taken and read at 535 nm using TECAN, infinite 200 Pro. The calculation was done using Lambert-Beer's law with path length 1 cm and molar extinction coefficient, $\epsilon = 1.56 \times 10^5$ /M/cm.

Protein carbonylation Protein carbonylation (PC) is one of the most harmful irreversible oxidative modifications of proteins which are promoted by excessive free radical generation. Oxidative modification of proteins occurs due to the derivatization of amino acid residues like proline, arginine, and lysine to reactive carbonyl derivatives. These reactive carbonyl derivatives can be measured by reaction with 2,4-dinitrophenyl hydrazine (DNPH) resulting in the formation of hydrazone which can be quantified by using a spectrophotometer (Levine et al. 1990). For this estimation, 100 mg of muscle tissue was homogenized in ice-cold 0.154 M KCL-EDTA buffer (pH 7.2) with protease inhibitor cocktail using Omni Tissue Homogenizer (Omni TH (220), Omni International, USA), keeping the tissue sample on ice. The homogenate was kept on ice for 10 min and then centrifuged at 10,000g for 15 min, and supernatant was collected in fresh tubes. To 500 μ l of supernatant, 500 μ l of 10 mM DNPH in 2 N HCl was added; 2 N HCl was taken as blank control. The mixture was incubated for 1 h at room temperature with vortexing every 15 min. The protein was then precipitated with an equal volume of 20% trichloroacetic acid (TCA) and was then centrifuged at 10,000 rpm for 5 min. The resulting pellet was washed thrice with ethanol/ethyl acetate (1:1 v/v). The final precipitate was then dissolved in 400 μ l of 6 M guanidine hydrochloride (pH 2.3) and kept at 37 °C for 15 min. The insoluble debris was removed by centrifugation. The absorbance of the DNPH derivatives was measured at 366 nm. The concentration of carbonyl groups was calculated using an absorbance coefficient 22,000/M/cm and expressed as nmol/mg protein.

Advanced oxidation protein products It is another reliable marker for protein oxidation, formed due to oxidative stress by reaction with chlorinated oxidants like hypochlorous acid and chloramines. Advanced oxidation protein products (AOPP) were measured using a method described by Witko-Sarsat et al. (1996). Briefly, 200 μ l of the tissue homogenate (diluted 1:5 times) was taken in 96-well plate and 10 μ l of

1.16 M potassium iodide was added. After incubation for 10 min at room temperature with continuous shaking, the reaction was stopped by 20 μ l of glacial acetic acid and reading was taken at 340 nm. The concentration was calculated using chloramines T standard curve.

Antioxidant status

Catalase This assay measures the decomposition of hydrogen peroxide by catalase enzyme present in the sample, which is evident from the decrease in absorbance at 240 nm (Beers and Sizer 1952). To 100 μ l of sample, 2.9 ml of substrate buffer (0.1% hydrogen peroxide in 50 mM sodium-potassium phosphate buffer, pH 7) was added and absorbance was measured at 240 nm for 3 min with 15 s interval. The concentration of catalase was calculated using the molar extinction coefficient 41/M/cm.

Superoxide dismutase The estimation of superoxide dismutase (SOD) in the sample was done using a previously established method (Marklund and Marklund 1974). This method is based on the principle of inhibitory effects of SOD on the reduction of NBT (nitrobluetetrazolium) dye by superoxide radicals, which are generated by pyrogallol. To 1.5 ml of 50 mM cacodylate buffer, 300 μ l of 1.0 mM NBT was added along with 10 μ l of 60 mM Pyrogallol. From this autooxidation of nitrobluetetrazolium (NBT) by superoxide radicals, being generated by pyrogallol was recorded. For measuring SOD activity in sample, 50 μ l of the sample was added to the above mixture. The absorbance of NBT was read at 540 nm for 3 min at 15 s intervals. Cacodylate buffer was taken as blank. Results were expressed as U/mg protein.

Glutathione peroxidase Glutathione peroxidase activity was measured in muscle homogenate using a commercially available kit following the manufacturer's instructions (EGPx-100, Bioassay systems; EnzyChrome glutathione peroxidase assay kit). The results were expressed as U/mg protein.

Reduced glutathione and oxidized glutathione The reduced glutathione (GSH) and oxidized glutathione (GSSG) levels were measured in soleus and gastrocnemius muscle homogenates according to the procedure followed by Hissin and Hilf (1976). In brief, 250 μ l of homogenate was taken, to which an equal volume of 10% metaphosphoric acid was added, followed by centrifugation at 10,000g for 30 min at 4 °C. The supernatant thus obtained was then used for estimation of GSH by incubation with o-phthalaldehyde and for GSSG by incubation with N-ethylmaleimide followed by o-phthalaldehyde reaction. Readings were taken at 350 nm excitation and 420 nm emission using a spectrofluorimeter (TECAN, infinite200pro). The amount of GSH and GSSG in respective muscles was expressed as μ mol/mg protein.

Intracellular-free calcium

The intracellular-free calcium was measured in the cytosolic fraction of tissue homogenate using a commercially available kit following the manufacturer's instructions (KA0812, Abnova). Briefly, 100 mg muscle tissue was homogenized in an ice-cold buffer (0.5 M sucrose, 10 mM HEPES, 10 mM KCl, 1.5 mM MgCl₂, 10% glycerol, 1 mM EDTA, 1 mM DTT, 1 mM PMSF fortified with protease inhibitors). Homogenates were kept on ice for 15 min, 0.6% Nonidet P-40 was added, and then centrifuged for 20 min at 5000 g at 4 °C. The supernatant with cytosolic fraction was collected in fresh tubes. To 25 µl of cytosolic fraction and standards, 90 µl of substrate buffer along with 60 µl of calcium assay buffer was added and mixed well in 96-well plate. The mixture was incubated for 10 min in dark. The absorbance was then taken at 577 nm. The concentration of intracellular free calcium was calculated using a standard curve and results were expressed as percentage change.

Histology

Animals were anesthetized using sodium pentobarbital (50 mg/kg body weight) and then were perfused with 0.1 M PBS (pH 7.4) followed by fixation with 4% paraformaldehyde. Further muscles were removed and kept in the same fixative overnight. Blocks were prepared using paraffin following dehydration, clearing, and wax impregnation. Five-micrometer sections of the tissue were cut using a microtome. Then, the tissue was stained with hematoxylin and eosin after deparaffinization with xylene. The morphology of muscle tissue was studied using digital images obtained with bright field microscopy at × 40 magnification using a Nikon eclipse, Ti2-E microscope.

Western blotting

Expressions of PERK, p-PERK, IRE-1α, p-IRE-1α, ATF-6, Bip, myoglobin, Caspase12, Caspase3, Caspase9, Bcl2, Bax, mTOR, and GAPDH in muscle homogenates were determined using western blot (appendix A). Forty-microgram protein was separated on SDS-polyacrylamide gel electrophoresis and transferred on PVDF membrane (Millipore). The membranes were then blocked with 3% bovine serum albumin (BSA) in phosphate-buffered saline (PBS) with 0.1% tween-20 at room temperature for 1 h. Membranes were then washed and probed with primary antibodies (as shown in table). After incubation, membranes were washed thrice followed by incubation with respective secondary antibodies. The membranes were then developed using a chemiluminescent substrate (Sigma) in Chemidoc (Biorad). Quantification was done by densitometry using ImageJ software.

In situ terminal deoxynucleotidyl transferase-mediated dUTP nick end-labeling

The terminal deoxynucleotidyl transferase-mediated dUTP nick end-labeling (TUNEL) assay was performed to detect DNA strand breaks for cell death. Briefly, 15-µm sections of muscle tissue were mounted on coated glass slides ($n = 3$ for each group). The dehydrated sections were then treated with 100 µl Proteinase K (Sigma). Sections were then dipped in 10% formalin, washed, and equilibrated with equilibration buffer for 7 min at RT (Promega, G327B). Following this, sections were incubated with the rTDT reaction mixture at 37 °C for 1 h. Washed sections were treated with 3% hydrogen peroxide for removal of endogenous peroxidase activity and then incubated with streptavidin HRP (1:500) for 30 min at RT. Sections were developed with DAB, counterstained, and cleared in xylene. They were mounted with DPX, covered with a coverslip, and examined for DNA damage under × 100 power (Nikon eclipse, Ti2-E microscope).

Statistical analysis

All experiments were performed in duplicates, and data are presented as mean ± SD. Two-way ANOVA with post hoc Tukey's test was used to determine statistical significance between groups. All analyses were conducted using GraphPad Prism version 8 software (GraphPad, CA, USA). The p value of ≤ 0.05, with a 95% confidence interval, was considered significant.

Results

Effect of heat stress on core, skin, and muscle temperature

Table 1 depicts the average core and skin temperature in rats exposed to thermoneutral and heat-stressed conditions. The rats exposed to heat stress (HS, 42 °C) showed a significant increase in core as well as skin temperature as compared to the control group post-exposure. The average initial core and skin temperature were comparable in both the groups but reached to 41.44 ± 0.45 °C ($p < 0.0001$) and 41.09 ± 0.37 °C ($p < 0.0001$) respectively in heat-stressed group after 1 h of exposure (Table 1). Muscle temperature of SL and GS was also measured after exposure in control as well as heat stressed groups. It was found to be increased remarkably in both the heat-stressed muscles in a similar fashion. Heat exposure resulted in a significant increase of ~ 1.27-fold ($p < 0.05$) and ~ 1.26-fold ($p < 0.05$) in soleus and gastrocnemius muscle respectively post-exposure (Fig. 1).

Table 1 Average core and skin temperature in rat control (C) and heat-stressed group (HS) pre- and post-exposure

	Control group (C)		Heat stressed group (HS)	
	Pre	Post	Pre	Post
Core temperature (°C)	36.74 ± 0.497	36.86 ± 0.481	36.96 ± 0.447	41.44 ± 0.450**
Skin temperature (°C)	24.85 ± 0.380	25.62 ± 0.466*	25.31 ± 0.523	41.09 ± 0.372**

Results are expressed as mean ± SD ($n = 8$). “*” indicates pre- vs post-temperature ($p < 0.005$); “**” indicates pre- vs post-group ($p < 0.0001$)

Heat stress-induced oxidative damage in soleus and gastrocnemius muscles

Free radical generation, protein oxidation (PC, AOPP), and lipid peroxidation (MDA) were measured as markers of oxidative stress (Fig. 2). Heat exposure resulted in increased production of free radicals in SL and GS muscles. A significant increase of 2.5-fold ($p < 0.05$) in free radical generation was measured in SL muscle whereas approximately 2.4-fold ($p < 0.05$) increase was recorded in GS muscle compared to respective control groups (Fig. 2a). However, the free radical generation in heat-stressed SL (SL HS) muscle was much higher than the heat-stressed GS (GS HS) muscle (~51%, $p < 0.05$) (Fig. 2a). Excessive free radicals generated after HS further react with proteins leading to the production of peptide fragments possessing highly reactive carbonyl groups and cause non-specific modification of lipids leading to dysfunction of normal cellular processes. Our data showed a remarkable increase in protein carbonyls as a marker protein oxidation in SL and GS muscles after heat exposure. As observed in Fig. 2b, heat exposure resulted in a 2.3-fold increment in SL ($p < 0.05$) and nearly 2-fold ($p < 0.05$) elevation in GS muscle compared to their respective controls. A

substantial increase of ~31% in protein carbonyl formation was observed in SL HS muscle as compared to GS HS muscle ($p < 0.05$). AOPP, another reliable marker of protein oxidation, also exhibited a similar trend. Following heat exposure, a significant upsurge of 1.8-fold in SL ($p < 0.05$) and 1.5-fold in GS muscle was seen as compared to control groups (Fig. 2c). When compared to the GS HS muscle, SL HS showed higher levels of AOPP but the difference was not significant (Fig. 2c). Furthermore, the levels of MDA as the marker of lipid peroxidation were measured after heat stress in the muscles and significant elevations were recorded (Fig. 2d). In SL muscle, ~49% increase was noted whereas in GS muscle nearly 38% rise was recorded ($p < 0.05$) in the HS group as compared to the control group. No significant differences in MDA levels were seen in SL HS and GS HS muscles (Fig. 2d).

Heat stress and muscle damage

Myoglobin expression was examined as a marker of heat-induced muscle damage using western blot, and a significant decrease (~5-fold, $p < 0.05$) in its protein level in SL HS muscle was observed as compared to SL C (Fig. 3a–b). GS HS muscle also showed a decline in myoglobin expression; however, the change was not significant. While comparing the SL HS and GS HS muscles, a ~27% decline in myoglobin expression was noted in SL HS compared to HS GS muscle. However, the difference was not significant (Fig. 3a–b).

Heat exposure-mediated changes in antioxidant status

Antioxidants form the first line of defense against oxidative stress. The levels of antioxidants, CAT, SOD, GPx, and glutathione, were measured in both the muscles to evaluate the effect of heat stress on their activity. As observed in Fig. 4a, the CAT activity was found to be increased significantly in both muscles after heat stress. In SL HS muscle, 52% ($p < 0.05$) increase in CAT activity was observed, whereas, in GS HS 25% ($p < 0.05$), hike was observed as compared to controls. However, the increase in CAT activity was much higher (~26%, $p < 0.05$) in SL HS than GS HS muscle (Fig. 4a). A significant increase of 47% ($p < 0.05$) in SOD enzyme

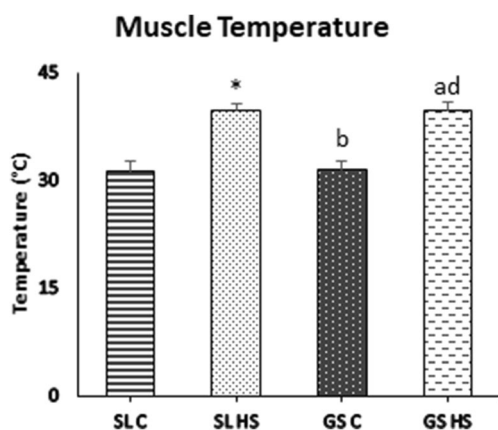


Fig. 1 Graph showing average muscle temperature in rat soleus and gastrocnemius muscles post-exposure. SL C soleus control group, SL HS soleus heat stress group, GS C gastrocnemius control group, GS HS gastrocnemius heat stress group; Result is expressed as mean ± SD. “*” indicates SL C vs SL HS group ($p < 0.05$). “a” indicates SL C vs GS HS group ($p < 0.05$). “b” indicates SL HS vs GS C group ($p < 0.05$). “d” indicates GS C vs GS HS group ($p < 0.05$)

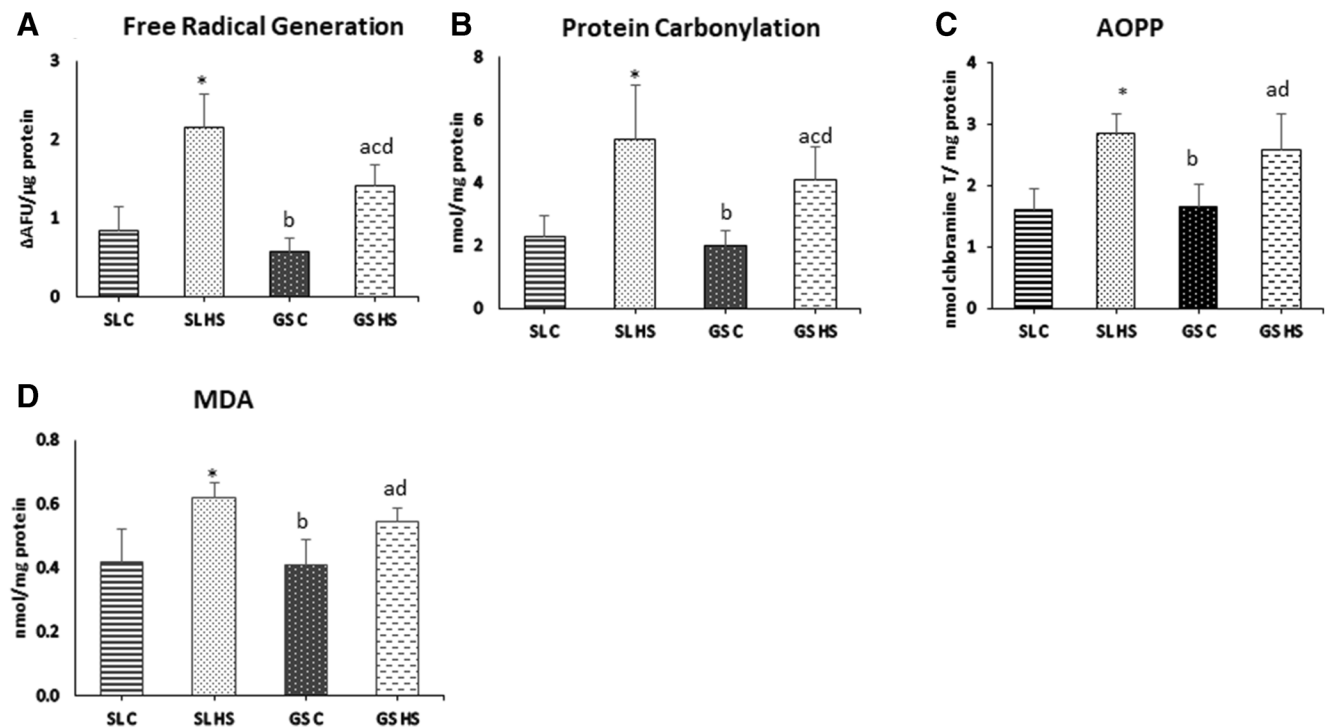


Fig. 2 Effect of heat stress on (a) free radical generation, (b) protein carbonylation, (c) AOPP, and (d) MDA in rat soleus and gastrocnemius muscles. SL C soleus control group, SL HS soleus heat stress group, GS C gastrocnemius control group, GS HS gastrocnemius heat stress group.

activity was registered in SL HS, and a 36% ($p < 0.05$) rise in GS HS muscle was noted as compared to the control group (Fig. 4b). No significant difference was recorded in the SOD activity of SL HS and GS HS muscle (Fig. 4b). GPx activity was also assessed in the muscle homogenates after heat stress. A significant increase of 62% ($p < 0.05$) in GPx was observed in SL HS muscle compared to SL C (Fig. 4c), whereas the increase in GPx activity in GS HS muscle was not significant (8%) as compared to GS C. SL HS muscle showed a 48%

Results are expressed as mean \pm SD. “*” indicates SL C vs SL HS group ($p < 0.05$). “a” indicates SL C vs GS HS group ($p < 0.05$). “b” indicates SL HS vs GS C group ($p < 0.05$). “c” indicates SL HS vs GS HS group ($p < 0.05$). “d” indicates GS C vs GS HS group ($p < 0.05$)

($p < 0.05$) increase in GPx activity compared to GS HS muscle (Fig. 4c). Furthermore, the levels of reduced and oxidized glutathione were also quantified in the muscle homogenates. A significant decrement in GSH (reduced glutathione) level was noticed, ~ fourfold in SL and ~ 1.8-fold in GS muscle as compared to control group muscles ($p < 0.05$) (Fig. 4d). The GSSG (oxidized glutathione) was found to be elevated significantly in both the muscle with 46% ($p < 0.05$) escalation in SL and 35% ($p < 0.05$) upsurge in GS compared to the control

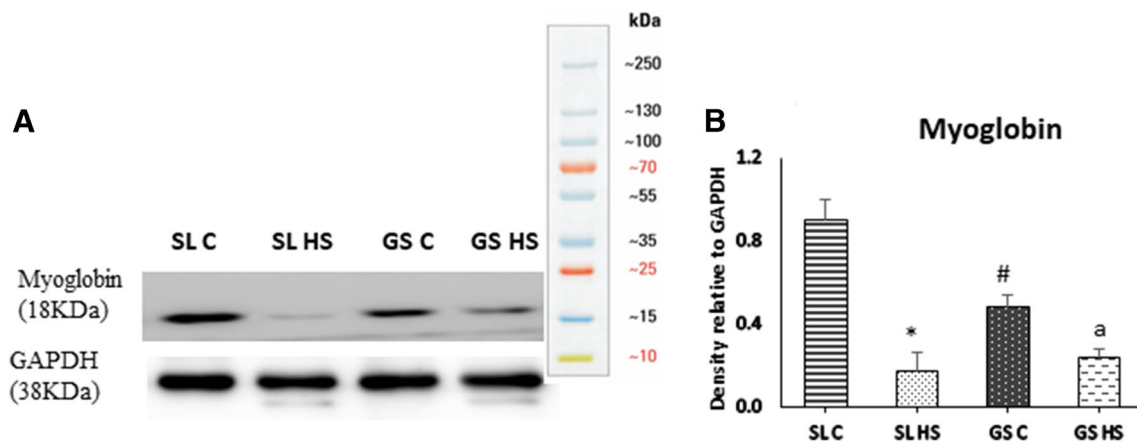


Fig. 3 a Western blot result for the expression of myoglobin in soleus (SL) and gastrocnemius (GS) muscles under thermoneutral (C) and heat-stressed condition (HS). b Densitometric quantification of western blot results. Protein levels were normalized to GAPDH. Data is presented as

mean \pm SD ($n = 3$ /group). “*” indicates SL C vs SL HS group ($p < 0.05$). “#” indicates SL C vs GS C group ($p < 0.05$). “a” indicates SL C vs GS HS group ($p < 0.05$)

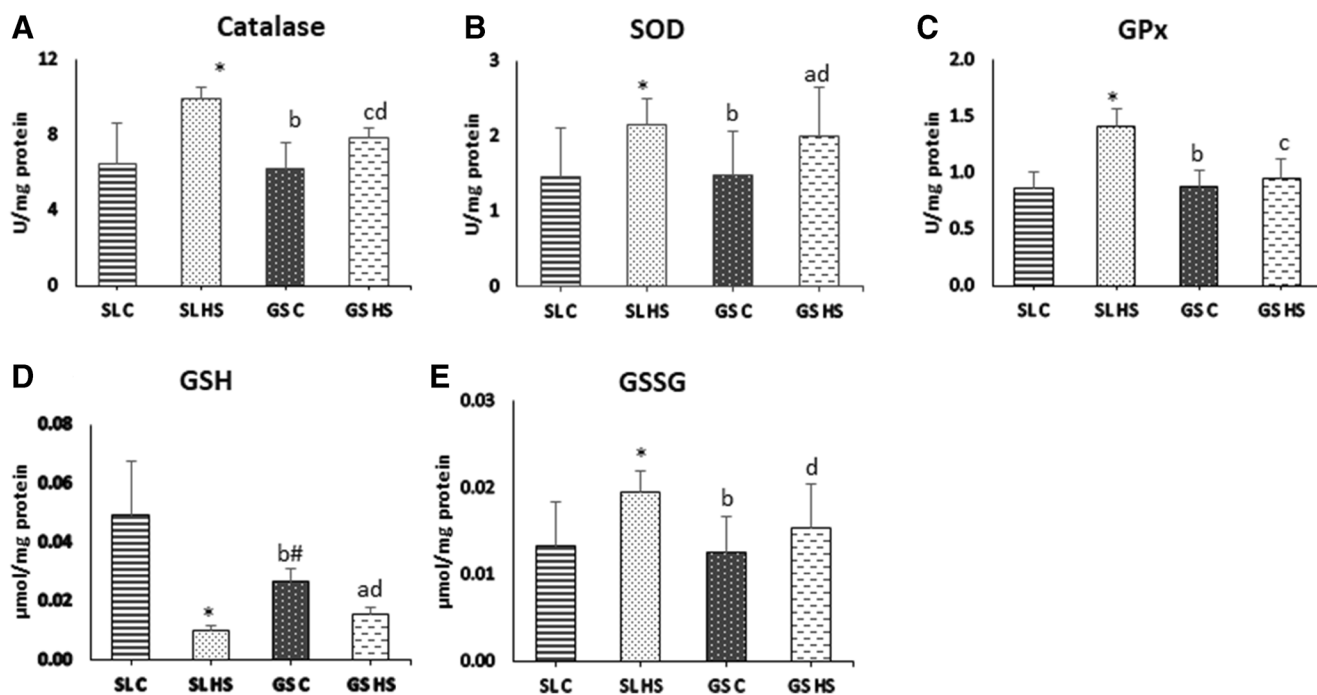


Fig. 4 Effect of heat stress on (a) catalase (CAT), (b) superoxide dismutase (SOD), (c) glutathione peroxidase (GPx), (d) reduced glutathione (GSH), and (e) oxidized glutathione (GSSG) in rat soleus and gastrocnemius muscles. SL C soleus control group, SL HS soleus heat stress group, GS C gastrocnemius control group, GS HS

gastrocnemius heat stress group. Results are expressed as mean \pm SD. “*” indicates SL C vs SL HS group ($p < 0.05$). “#” indicates SL C vs GS C group ($p < 0.05$). “a” indicates SL C vs GS HS group ($p < 0.05$). “b” indicates SL HS vs GS C group ($p < 0.05$). “c” indicates SL HS vs GS HS group ($p < 0.05$). “d” indicates GS C vs GS HS group ($p < 0.05$)

group (Fig. 4e). No significant differences in GSH and GSSG levels were found between SL HS and GS HS (Fig. 4d–e).

Effect of heat stress on calcium homeostasis

Calcium is an important ion playing a crucial role in various cellular processes like muscle contraction. As observed in Fig. 5, exposure to heat stress results in a significant increase in intracellular calcium levels in SL HS muscle as compared to SL C (fourfold ($p < 0.05$)). While in GS muscle, non-

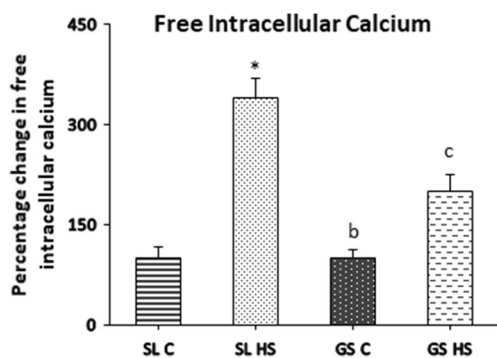


Fig. 5 Effects of heat stress on free intracellular calcium in rat soleus and muscles. SL C soleus control group, SL HS soleus heat stress group, GS C gastrocnemius control group, GS HS gastrocnemius heat stress group. Results are expressed as mean \pm SD. “*” indicates SL C vs SL HS group ($p < 0.05$). “b” indicates SL HS vs GS C group ($p < 0.05$). “c” indicates SL HS vs GS HS group ($p < 0.05$)

significant elevation was observed (Fig. 5) following heat exposure as compared to the control group. When compared to the GS HS muscle, SL HS muscle showed \sim twofold ($p < 0.05$) increment in intracellular calcium levels (Fig. 5).

Effects of heat stress on histological aspects

The histopathology of SL and GS muscles was also examined to evaluate the effects of heat-induced alterations in the muscles. Sections of SL and GS from both the control and heat-stressed groups were stained with H & E and observed under $\times 40$ magnification. The SL muscle sections from control group rats showed transverse cut muscle fibers with uniform shape and size, peripherally located nuclei and abundant myofibrils within individual myofibers, evenly separated by extracellular space (Fig. 6a). The muscle sections from the control group of GS muscle also showed a similar arrangement of muscle fibers (Fig. 6c). However, the heat stress-exposed group SL muscle section showed heterogeneous size and shape. Some myofibers were round and big while some were quite small. Some of the muscle fibers also showed internalized nuclei indicating re/degeneration of myofibers (indicated by arrows) (Fig. 6b). The extracellular space between individual muscle fibers was quite large as compared to the control group (indicated by double-headed arrows) (Fig. 6b). Splitting of the sarcolemma and apparent degradation of muscle fibers were also evident in the sections (indicated by the white

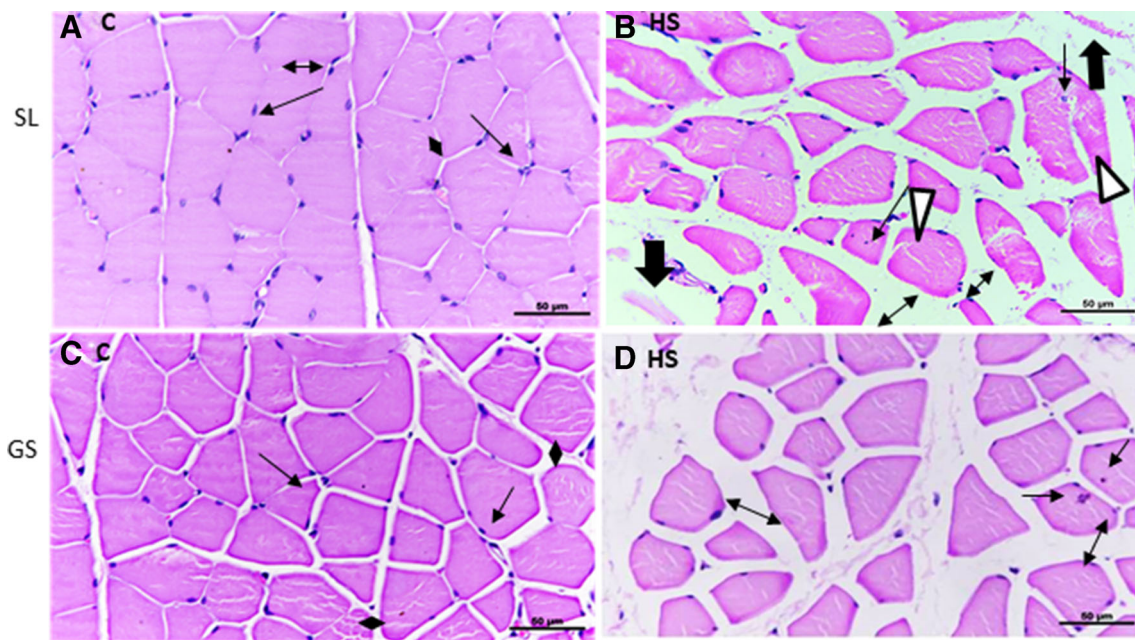


Fig. 6 Transverse sections of soleus (SL) and gastrocnemius (GS) under thermoneutral (25 °C, control (C)) and heat-stressed conditions (HS, 42 °C for 1 h). **a** Transverse section of control soleus (SL C) muscles showing myofibers with homogenous size, polygonal shape with peripheral nuclei with intact sarcolemma, and sarcoplasm. **b** Transverse section of heat-stressed soleus muscles (SL HS) with unevenly shaped fibers, some with internally located nuclei hinting at repeated cycles of degeneration and regeneration, also shows split sarcolemma and degenerating cells. **c** Transverse section of control gastrocnemius (GS C) showing

homogenously distributed myofibers with homogeneous diameter, polygonal shape with peripheral nuclei, and intact structure. **d** Transverse section of heat-stressed gastrocnemius muscle (GS HS) showing heterogeneously shaped myofibers, some small and some big. Arrow (\rightarrow) showing nuclei, Thick arrow (Ψ) showing degenerating myofibers. White triangle (Δ) showing disrupted sarcolemma. Double-headed arrow (\leftrightarrow) represents the space between myocytes. The scale bar at the bottom represents 50 μm

triangle) (Fig. 6b). GS HS muscle sections also revealed variability in size and shape of fibers, some showing internally located nuclei (indicated by arrows) and increased extracellular space between muscle fibers (indicated by two-headed arrow) (Fig. 6d). Furthermore, the cross-sectional area (CSA) was also examined in both muscles. As depicted in Fig. 7, SL HS muscle showed a significant reduction in myofiber's size as compared to control ($\sim 26\%$, $p < 0.05$) as well as GS HS muscle fibers ($\sim 24\%$, $p < 0.05$). The change in CSA in GS HS muscle fibers was not significant compared to control (Fig. 7). Thus, it is evident that heat stress has more damaging effects in SL than GS muscle.

Effect of heat exposure on ER stress and UPR

Heat stress induces oxidative damage in muscle cells and leads to ER stress. To assess the effects of heat stress on ER and UPR pathway, the three transducer proteins PERK, IRE-1 α , and ATF-6 were analyzed using western blot (Fig. 8a). Following heat exposure, a significant increase of twofold ($p < 0.05$) was noted in the expression of PERK in SL HS, while no significant change was seen in GS HS as compared to GS C. No considerable change was noted while comparing SL HS and GS HS muscles (Fig. 8b). A significant increase in the phosphorylated levels of PERK was observed in SL HS (\sim

threefold, $p < 0.05$) and GS HS (~ 1.5 -fold, $p < 0.05$) as compared to their respective control groups with the insignificant difference among the SL HS and GS HS muscles (Fig. 8c). IRE-1 α and its phosphorylated form (p-IRE-1 α) showed marked upregulation in SL HS (\sim twofold and \sim fourfold, respectively, $p < 0.05$) as compared to control group muscles, SL C (Fig. 8d–e). No significant change in IRE-1 α and its

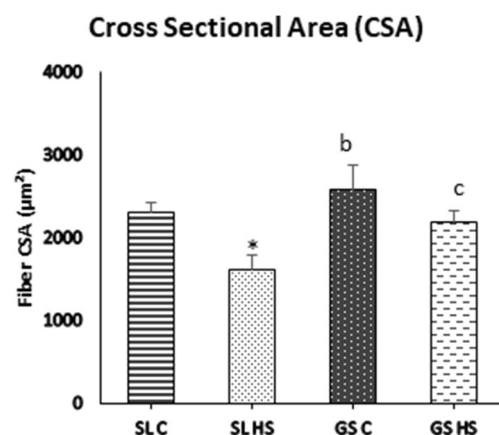


Fig. 7 Cross-sectional area (CSA) of fibers in soleus (SL) and gastrocnemius (GS) under thermoneutral condition (C) and heat-stressed condition (HS), respectively. Results are expressed as mean \pm SD. “*” indicates SL C vs SL HS ($p < 0.05$). “b” indicates SL HS vs GS C group ($p < 0.05$). “c” indicates SL HS vs GS HS group ($p < 0.05$)

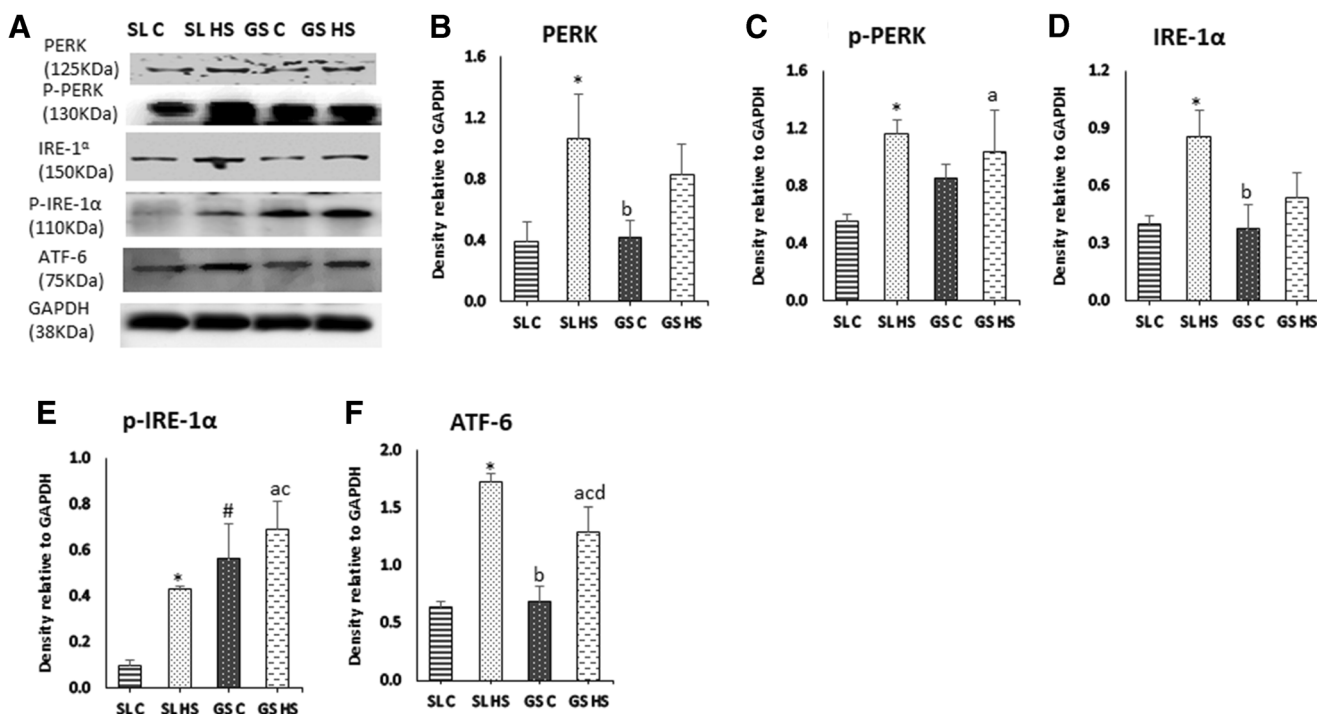


Fig. 8 a Western blot result for the expression of ER membrane-associated proteins; PERK, p-PERK, IRE-1 α , p-IRE-1 α , and ATF-6, in soleus (SL) and gastrocnemius (GS) muscles under thermoneutral (C) and heat-stressed conditions (HS). b–f Densitometric quantification of western blot results. Protein levels were normalized to GAPDH. Data are

presented as mean \pm SD ($n=3$ /group). “*” indicates SL C vs SL HS group ($p < 0.05$). “#” indicates SL C vs GS C group ($p < 0.05$). “a” indicates SL C vs GS HS group ($p < 0.05$). “b” indicates SL HS vs GS C group ($p < 0.05$). “c” indicates SL HS vs GS HS group ($p < 0.05$). “d” indicates GS C vs GS HS group ($p < 0.05$)

phosphorylated form was observed in GS HS compared to GS C (Fig. 8d–e). However, the expression of p-IRE-1 α was significantly higher in GS C as compared to SL C (~fivefold, $p < 0.05$). Similarly, p-IRE-1 α levels were significantly elevated in GS HS muscle compared to SL HS muscle (~1.7-fold, $p < 0.05$) (Fig. 8e). The third sensor of ER stress is ATF-6, another transmembrane protein whose levels were also found to be profoundly elevated in both the muscles following heat exposure (Fig. 8f). Around 2.6-fold ($p < 0.05$) upsurge was noted in SL HS and 1.8-fold ($p < 0.05$) increase in GS HS muscles compared to their respective control group muscles (Fig. 8f). A significant increase of ~1.5-fold ($p < 0.05$) in ATF-6 expression was also recorded in SL HS when compared to GS HS muscle (Fig. 8f). All these sensor proteins of ER stress help in restoring equilibrium by increasing the expression of ER chaperone and UPR pathway proteins, to relieve ER stress. Furthermore, the expression of Grp 78 a resident ER chaperone was evaluated (Fig. 9a) and was found to be markedly elevated in SL HS (82%, $p < 0.05$) as compared to SL C. However, GS HS showed a non-significant change as compared to GS C (Fig. 9c). Besides, the expression of mTOR a regulator of protein synthesis was also examined using western blot (Fig. 9a) and it was found to be downregulated in SL HS as well as GS HS muscle significantly compared to SL C and GS C, respectively (~40% in both the muscles, $p < 0.05$) (Fig. 9c). However, no significant

difference in mTOR expression was noted among HS SL and HS GS muscle (Fig. 9c). mTOR is a promoter of protein translation but its expression was found to be significantly downregulated in both the muscles after heat exposure. The decrease in mTOR expression in SL HS and GS HS muscles indicates attenuation in the protein translation mediated by UPR responsive genes to control ER stress.

Apoptotic signaling cascade under heat stress

When the UPR pathway fails to resolve the ER stress, apoptosis eventuates. The expression of CHOP and caspase12 associated with ER stress was examined using western blotting (Fig. 10a). The expression levels of both CHOP and caspase12 were significantly higher in SL (~2.7-fold and ~2.3-fold, respectively, $p < 0.05$) while insignificant in GS after heat exposure as compared to their respective control muscles (Fig. 10b–c). Also, the SL HS showed a significant increase in the expression of CHOP (~twofold, $p < 0.05$) as well as Caspase12 (~1.8-fold, $p < 0.05$) compared to GS HS muscle (Fig. 10b–c).

Apoptosis plays a pivotal role in regulating muscle mass. To explore underlying mechanisms of apoptosis under heat stress in skeletal muscle, expression levels of Caspase9, caspase3, Bcl2, and Bax were estimated using western blot (Fig. 11a). Caspase9 was significantly upregulated in SL HS

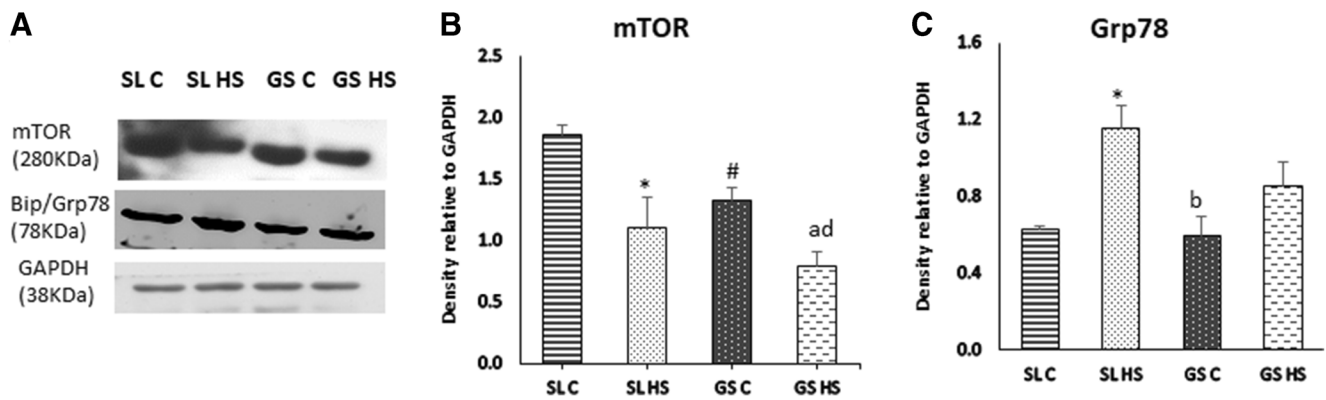


Fig. 9 a Western blot result for the expression of mTOR a regulatory protein synthetic pathway and Grp78 an ER chaperone in soleus (SL) and gastrocnemius (GS) muscles under thermoneutral (C) and heat-stressed conditions (HS). b–c Densitometric quantification of western blot result. Protein levels were normalized to GAPDH. Data are presented as mean \pm

SD ($n = 3/\text{group}$). “*” indicates SL C vs SL HS group ($p < 0.05$). “#” indicates SL C vs GS C group ($p < 0.05$). “a” indicates SL C vs GS HS group ($p < 0.05$). “b” indicates SL HS vs GS C group ($p < 0.05$). “d” indicates GS C vs GS HS group ($p < 0.05$)

muscle (~ 2.5 -fold, $p < 0.05$) compared to SL C and ($\sim 32\%$, $p < 0.05$) compared to GS HS muscle, while no significant change was seen in GS HS compared to GS C (Fig. 11b). Caspase3 was found to be significantly elevated in HS SL (~ 2.5 -fold ($p < 0.05$)) while non-significantly in HS GS muscle compared to SL C and GS C, respectively (Fig. 11c). No significant difference was seen in SL HS compared to GS HS muscle. A remarkable decrement in Bcl2 expression was seen in SL HS ($\sim 50\%$, $p < 0.05$) compared to SL C (Fig. 11d). Bcl2 expression was also found to be non-significantly downregulated in GS HS muscle compared to GS C (Fig. 11d). Also, no significant difference was found between SL HS and GS HS muscle (Fig. 11d). The level of Bax a pro-apoptotic protein was found to be increased significantly in both the muscles following heat stress (Fig. 11e). An increase of \sim threefold ($p < 0.05$) was observed in SL HS as compared to SL C and ~ 1.5 -fold ($p < 0.05$) increase was observed in GS HS as compared to GS C (Fig. 11e). Also, in SL HS muscle, the increase in Bax expression was much higher than GS HS muscle (~ 1.5 -fold ($p < 0.05$)) (Fig. 11e). As observed in our results, the

SL muscle showed a marked increase in apoptotic markers than GS muscle after exposure to heat stress. The above results were confirmed from the TUNEL assay (Fig. 12a–e). TUNEL assay clearly showed a greater number of TUNEL-positive nuclei (indicated by black arrow) in SL HS muscle as compared to SL C and GS HS muscle (Fig. 12a–e). As depicted in Fig. 12e, SL HS muscle showed a significant increase of ~ 2.8 -fold ($p < 0.05$) and ~ 1.7 -fold ($p < 0.05$) in apoptotic nuclei as compared to SL C and GS HS, respectively. No significant change in apoptotic nuclei was found in GS HS muscle compared to GS C muscle (Fig. 12e).

Discussion

Heat stress is well known to cause deleterious effects in humans as well as in animals (St-Pierre et al. 2003). However, little is known about heat stress-mediated biochemical alterations in skeletal muscles. HS has been shown to negatively impact muscle growth raising the possibility of dysfunction and decrement

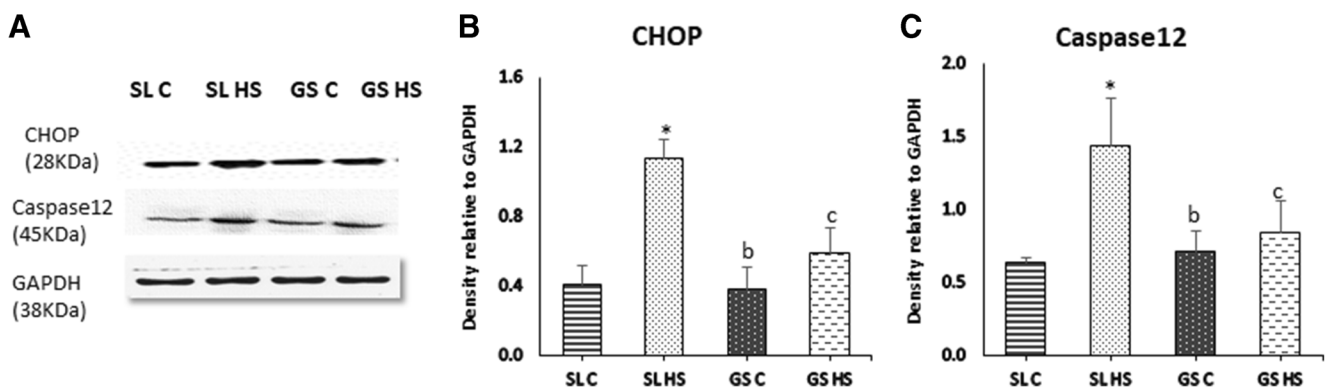


Fig. 10 a Western blot result for the expression of markers of ER-induced apoptosis; CHOP and Caspase 12 in soleus (SL) and gastrocnemius (GS) muscles under thermoneutral (C) and heat-stressed conditions (HS). b–c Densitometric quantifications of western blot result. Protein

levels were normalized to GAPDH. The data are presented as mean \pm SD ($n = 3/\text{group}$). “*” indicates SL C vs SL HS group ($p < 0.05$). “b” indicates SL HS vs GS C group ($p < 0.05$). “c” indicates SL HS vs GS HS group ($p < 0.05$)

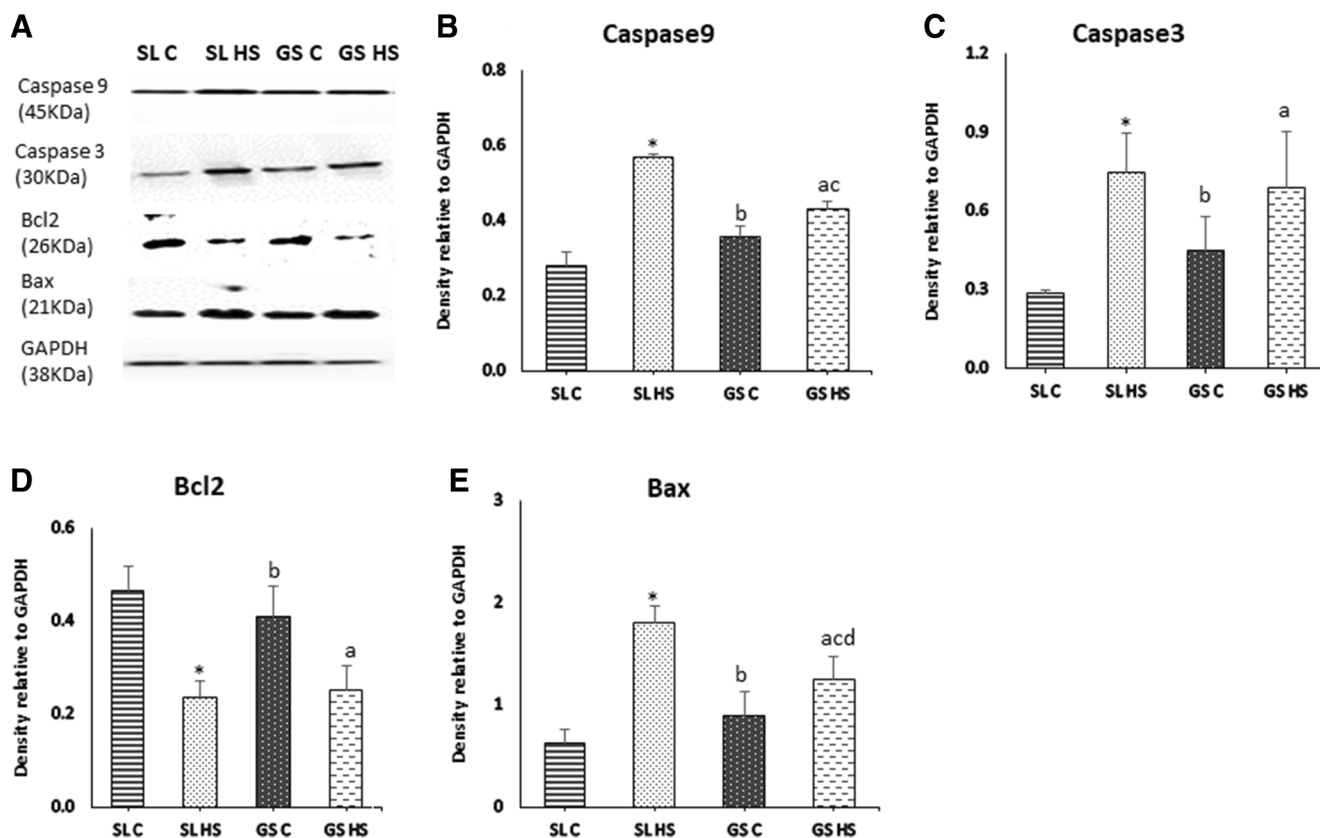


Fig. 11 **a** Western blot result for the expression of apoptotic pathway protein; Caspase-9, Caspase-3, Bcl2, and Bax in soleus (SL) and gastrocnemius (GS) muscles under thermoneutral (C) and heat-stressed conditions (HS). **b–e** Densitometric quantification of western blot results. Protein levels were normalized to GAPDH. Data are presented as mean

\pm SD ($n = 3/\text{group}$). “*” indicates SL C vs SL HS group ($p < 0.05$). “#” indicates SL C vs GS C group ($p < 0.05$). “a” indicates SL C vs GS HS group ($p < 0.05$). “b” indicates SL HS vs GS C group ($p < 0.05$), “c” indicates SL HS vs GS HS group ($p < 0.05$), “d” indicates GS C vs GS HS group ($p < 0.05$)

in performance due to increased heat load. Therefore, it is necessary to study the heat-mediated alterations in skeletal muscle pathology to devise mitigation strategies. The present study depicted the effects of heat stress on oxidative (soleus; SL) and glycolytic (gastrocnemius; GS) skeletal muscles. SL and GS form the calf muscles and vary in their fiber type composition. The role of these two muscles in various physical activities is undeniable (Alrowayeh et al. 2011). SL is composed predominantly of type 1 (oxidative/slow-twitch muscle fibers) fibers (~80–90%) while GS is a mixture of type 1 and type 2 fibers with a dominance of type 2 fibers (fast-twitch/glycolytic fibers, ~60–70%) (Gollnick et al. 1974; Wang et al. 2004). In addition to compositional differences, these two muscles also differ in their roles. The soleus muscle is majorly responsible for walking and maintaining posture and long-distance runs while the gastrocnemius muscle predominantly functions in sprinting and running. Due to these functional and compositional differences, these two muscles were chosen for the study. Both the muscles displayed several HS-induced physiological, morphological, and biochemical changes after heat exposure. However, SL and GS muscles showed a differential response to heat-induced ER stress.

The purpose of the study was to examine the effects of acute heat exposure on SL and GS muscles; for that, animals were exposed to HS in simulated conditions for 1 h. A significant rise in core, skin, and muscle temperature was recorded following heat exposure. Elevated core and muscle temperature have been shown to cause alterations in calcium release and its reuptake by sarcoplasmic reticulum and excessive free radical generation leading to oxidative stress (McAnulty et al. 2005). Several studies have shown that altered calcium release and oxidative stress might be associated with a reduced physical performance by decreasing force production or enhancing muscle fatigue (Moopanar and Allen 2006; Powers and Jackson 2008).

Our results showed increased production of free radicals in SL and GS muscles after exposure to heat stress. There are many potential sources of free radical formation in muscles, but mitochondria are considered as the major source due to progressive mitochondrial uncoupling and superoxide formation. Our results also suggest that increase in free radical generation after heat exposure causes protein oxidation. With protein oxidation, there is an incremental increase in protein carbonyl content and AOPP. Increased protein carbonyl

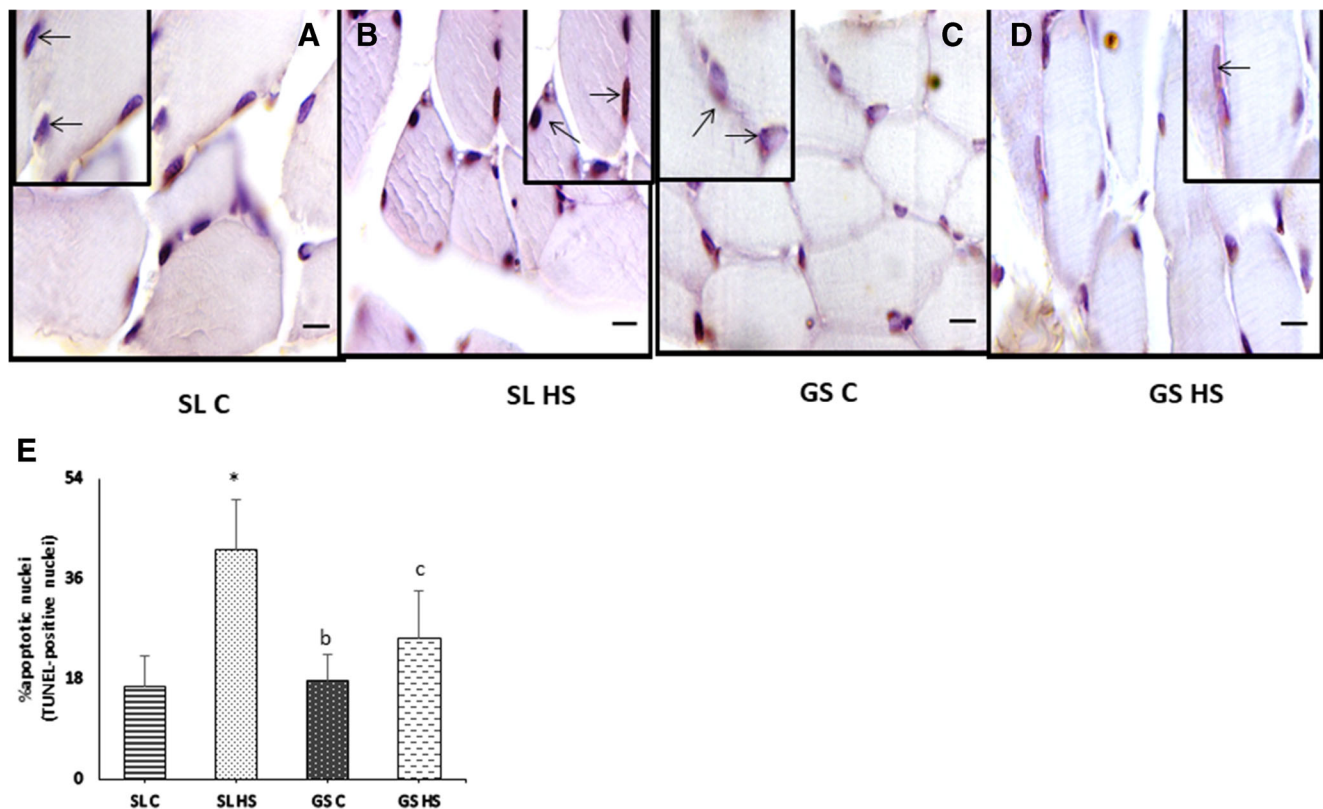


Fig. 12 Detection of apoptosis by terminal deoxynucleotidyl transferase-mediated dUTP nick end-labeling (TUNEL) in soleus (SL) and gastrocnemius (GS) muscle scale bar, 20 μ m. (a) Control soleus muscle (SL C). (b) Heat-stressed soleus muscles (SL HS). (c) Control gastrocnemius muscle (GS C). (d) Heat-stressed gastrocnemius muscle (GS HS). Apoptotic nuclei (black arrows) are more prominent in heat-stressed soleus muscle (SL HS) than the heat-stressed gastrocnemius muscle (GS

HS) as compared to their respective controls (SL C and GS C). (e) The apoptotic rate was expressed as the percentage of TUNEL-positive nuclei per total nuclei (apoptotic plus non-apoptotic nuclei). Results are expressed as mean \pm SD. “*” indicates SL C vs SL HS group ($p < 0.05$). “b” indicates SL HS vs GS C group ($p < 0.05$). “c” indicates SL HS vs GS HS group ($p < 0.05$)

content can result from direct oxidation of amino acids like lysine, arginine, histidine, proline, glutamic acid, and threonine in the peptide chain (Butterfield and Stadtman 1997; Castegna et al. 2003). Concurrent with an increase in free radical generation and protein oxidation, our results also depicted an increase in lipid peroxidation as indicated by levels of MDA in both the muscles. However, the heat exposure-mediated oxidative stress is more pronounced in soleus than gastrocnemius muscle. SL HS muscle showed a greater increase in the levels of all the oxidative stress parameters in the study compared to HS GS muscle. Particularly, the levels of free radicals and PC were significantly higher in HS SL muscle compared to GS HS (Fig. 3). These observations can better be explained as SL being almost entirely composed of oxidative muscle fibers and having a greater proportion of mitochondria than GS muscle. Mitochondria are regarded as the biggest source of free radicals with superoxide radicals being produced at complexes I and III of the electron transport chain (ETC). Mujahid et al. (2007) in their study have shown excessive generation of free radicals after acute HS (34 $^{\circ}$ C, 6 h, 12 h, and 18 h) resulting from increased mitochondrial respiration and beta oxidation due to enhanced energy demand

by the cells at the initial phase of heat stress. Exposure to HS also results in downregulation of uncoupling proteins (UCP) in mitochondria which further escalates free radical production (Mujahid et al. 2006). Whereas, GS muscle possesses fewer mitochondria and majorly relies on the glycolytic pathway for energy production. Several studies have advocated that heat stress alters cellular metabolism by enhancing glycolysis (Zhang et al. 2012; Baumgard and Rhoads 2013). Thus, the type 2 fibers that solely rely on the glycolytic pathway continue to produce energy to meet the enhanced demands while the oxidative phosphorylation in type I fibers is compromised.

Increased oxidative load under heat stress is believed to cause damage to the muscle cell membrane and disrupts membrane integrity by attacking polyunsaturated fatty acid lipid residues (Trachootham et al. 2008). In our study, a significant decrease in protein levels of myoglobin, an indicator of muscular damage, was found in SL muscle following heat exposure. It suggests disruption of skeletal muscle membrane integrity in soleus muscle following heat exposure. However, the decrease in gastrocnemius muscle was not significant. Myoglobin is a hemoprotein abundantly present in type 1

fibers. SL muscle being an oxidative muscle has a greater proportion of myoglobin than GS muscle. Myoglobin acts as an oxygen store and facilitates oxygen diffusion in muscle cells at the onset of muscle contraction (Masuda et al. 2013). Disruption of skeletal muscle membrane integrity decreases the myoglobin levels and thus, oxygen availability to contracting muscles. Also, the pro-oxidant environment further impairs the oxygen-binding ability of myoglobin (Montilla et al. 2014). Hence, the oxygen delivery to mitochondria and to contracting muscles is impaired resulting in compromised oxidative phosphorylation in SL HS muscle leading to muscle damage. Besides, SL and GS muscles were also examined for histopathological changes, which revealed greater damage in SL HS muscle as compared to GS HS. These observations further suggest that HS causes more damage to the soleus muscle as compared to the gastrocnemius muscle.

Oxidative stress occurs when there is a presence of excessive free radicals than the available antioxidants in the cell. To relieve oxidative stress, skeletal muscles are equipped with enzymatic antioxidants (Powers et al. 2011). The levels of CAT, SOD, and GPx were upregulated in both muscles after heat stress but the levels of CAT and GPx were significantly higher in SL HS than GS HS muscle. Also, the decline in GSH level and increase in GSSG level was more in SL HS than GS HS muscle. Antioxidants form the first line of defense against oxidative stress and increase in response to stress. However, excessive free radical formation along with protein modification causes an overload of misfolded proteins in muscle cells after heat exposure as shown in our study as well as previous studies (Fujii et al. 2018). Furthermore, increased free radicals cause an imbalance in cellular redox status and increase influx of calcium from ER. This increased influx of calcium from ER disrupts its homeostasis and results in ER stress (Ermak and Davies 2002; Davidson and Duchon 2006; Zima and Blatter 2006). As observed in our results, a significant increase in intracellular calcium was recorded in soleus muscle as compared to gastrocnemius muscle following heat exposure. Increased cytoplasmic calcium also exacerbates oxidative stress (Horimoto et al. 2006); this could be another reason for excessive damage in SL HS compared to GS HS.

To resolve ER stress, the unfolded protein response (UPR) pathway is activated. To further evaluate ER stress, Grp78/Bip, an ER-resident chaperone, was examined using western blot in both the muscles. The expression of Bip was found to be markedly elevated in soleus muscle as compared to gastrocnemius post-exposure suggesting an enhanced ER stress in soleus muscle following heat stress. All three transducers of the UPR pathway, PERK, ATF-6, and IRE-1 α , were assessed using western blot. The expression of PERK and p-PERK was significantly upregulated in soleus but not in gastrocnemius following heat stress compared to control. PERK on activation attenuates protein synthesis and prevent the influx of newly

formed proteins in the stressed ER compartment. Our results showed a significant reduction in mTOR expression after HS in both the muscles indicating a reduction in protein synthesis. PERK also activates genes involved in ER-mediated apoptosis. IRE-1 α and p-IRE1 α were also remarkably elevated in SL as compared to GS muscle after heat exposure compared to respective control groups. An inconsiderable change was seen in the GS HS muscle compared to GS C muscle. This signal transducer after activation promotes the upregulation of genes involved in the UPR and ERAD pathway to restore ER homeostasis and confer cytoprotection. It also activates apoptotic pathway genes if ER stress is prolonged. However, the GS C muscle showed a high expression of p-IRE-1 α compared to the SL C muscle. The GS C muscle also showed elevated levels of p-PERK when compared to SL C muscle; however, the difference was not significant. The elevated levels of these proteins in GS C muscle might be the reasons for the low impact of heat load on ER stress in GS muscle. These proteins are responsible for managing the protein turnover rate in stressed ER by controlling protein synthesis and degradation rate of unfolded and accumulated proteins in the ER. Already elevated levels of p-IRE-1 α and p-PERK in gastrocnemius muscle act quickly to restore ER homeostasis on exposure to heat stress. The levels of ATF-6 were found to be significantly upregulated in both the muscles, but more in SL HS compared to GS HS muscle. Dissociation of ATF-6 from Bip/Grp78 leads to its translocation to Golgi where it gets activated and induces the transcription of ER chaperones like Bip, to restore ER homeostasis. Our study showed that in SL HS, UPR fails to resolve ER stress. Hence, the signaling switches from pro-survival to pro-death, triggering ER stress-induced apoptosis, or cell death. This is evident from the significant upregulation of CHOP and Caspase12 in SL HS compared to GS HS.

CHOP, a downstream effector protein stimulated by PERK, favors apoptosis by decreasing expression of Bcl2. The expression of Bcl2 was significantly downregulated in SL muscle. Furthermore, expression of Caspase12, an ER-resident caspase, proposed as a mediator of ER stress-induced apoptosis, was significantly elevated in SL HS muscle. Activated Caspase12 then activates Caspase9 which ultimately activates Caspase3 and leads to apoptosis (Morishima et al. 2002; Boyce and Yuan 2006). As depicted in our results, the expressions of Caspase3, Caspase9, and Bax, pro-apoptotic proteins, were profoundly increased in SL HS as compared to GS HS following heat exposure. Induction of IRE-1 α has also been implicated in direct activation of Bax in ER-mediated apoptosis (Iurlaro and Muñoz-Pinedo 2016). The role of Bax has also been reported in ER calcium-mediated apoptosis along with Bak. The results of western blotting were then confirmed with TUNEL assay, which also showed a marked increase in apoptotic nuclei in SL than GS muscle following heat exposure. Increased apoptosis has also been linked to muscle mass loss and myofiber degeneration

(Dupont-Versteegden 2006) which is demonstrated with the histological findings in HS SL, which showed significantly decreased myofiber CSA compared to control as well as GS HS muscle. The results suggest that SL being an oxidative muscle is more susceptible to heat-induced ER stress, which triggers ER-mediated apoptosis through Caspase12 and CHOP activation.

In conclusion, the present study provides detailed insight into the effect of heat exposure on ER and individual arm of the UPR pathway in regulation of soleus and gastrocnemius muscle pathology. Overall, a higher oxidative load was observed in soleus muscle as compared to gastrocnemius muscle following heat exposure which could be associated with heat stress-induced enhanced intracellular calcium level in type I muscle fiber. Oxidative load then led to ER stress in both the muscle and caused activation of the UPR pathway. The expression of the sensor proteins was found to be significantly increased in SL HS muscle. The present study showed that heat exposure led to more severe ER stress in the soleus muscle with minor effects on gastrocnemius muscle. The severity of ER stress led to the failure of UPR and activation of apoptosis in SL HS muscle via activation of CHOP and caspase12. Overall, the present study depicted that soleus, majorly being an oxidative muscle, is more prone to heat stress-induced insult. Our study provides a clear pathway of excessive free radical production, ER stress to muscle mass loss due to enhanced apoptosis in HS SL muscle. This study extends our understanding of skeletal muscle response with different fiber type compositions under heat stress.

Supplementary Information The online version contains supplementary material available at <https://doi.org/10.1007/s12192-020-01178-x>.

Acknowledgments The authors are grateful to the Director, Defence Institute of Physiology and Allied Sciences, Delhi, for providing facilities to carry out these investigations.

Funding This study was supported and funded by the Defence Research and Development Organization, Ministry of Defence, Government of India.

Compliance with ethical standards

Competing interests The authors declare that there are no conflicts of interest.

References

- Adams CJ, Kopp MC, Larburu N, Nowak PR, Ali MMU (2019) Structure and molecular mechanism of ER stress signaling by the unfolded protein response signal activator IRE1. *Front Mol Biosci* 6: 11
- Agrawal A, Rathor R, Suryakumar G (2017) Oxidative protein modification alters proteostasis under acute hypobaric hypoxia in skeletal muscles: a comprehensive in vivo study. *Cell Stress Chaperones* 22: 429–443. <https://doi.org/10.1007/s12192-017-0795-8>
- Allen DG (2009) Fatigue in working muscles. *J Appl Physiol* 106:358–359
- Alrowayeh HN, Sabbahi MA, Etnyre B (2011) Similarities and differences of the soleus and gastrocnemius H-reflexes during varied body postures, foot positions, and muscle function: multifactor designs for repeated measures. *BMC Neurol* 11:65. <https://doi.org/10.1186/1471-2377-11-65>
- Altan Ö, Pabuçcuoğlu A, Altan A et al (2003) Effect of heat stress on oxidative stress, lipid peroxidation and some stress parameters in broilers. *Br Poult Sci* 44:545–550. <https://doi.org/10.1080/00071660310001618334>
- Azad MAK, Kikusato M, Sudo S, Amo T, Toyomizu M (2010) Time course of ROS production in skeletal muscle mitochondria from chronic heat-exposed broiler chicken. *Comp Biochem Physiol - A Mol Integr Physiol* 157:266–271. <https://doi.org/10.1016/j.cbpa.2010.07.011>
- Baumgard LH, Rhoads RP (2013) Effects of heat stress on postabsorptive metabolism and energetics. *Annu Rev Anim Biosci* 1:311–337. <https://doi.org/10.1146/annurev-animal-031412-103644>
- Beers RF, Sizer IW (1952) A spectrophotometric method for measuring the breakdown of hydrogen peroxide by catalase. *J Biol Chem* 195: 133–140. <https://doi.org/10.1093/jxb/48.2.181>
- Boyce M, Yuan J (2006) Cellular response to endoplasmic reticulum stress: a matter of life or death. *Cell Death Differ* 13:363–373
- Buege JA, Aust SD (1978) Microsomal lipid peroxidation. *Methods Enzymol* 52:302–310. [https://doi.org/10.1016/S0076-6879\(78\)52032-6](https://doi.org/10.1016/S0076-6879(78)52032-6)
- Butterfield DA, Stadtman ER (1997) Chapter 7 protein oxidation processes in aging brain. *Advances in Cell Aging and Gerontology* 2:161–191. [https://doi.org/10.1016/S1566-3124\(08\)60057-7](https://doi.org/10.1016/S1566-3124(08)60057-7)
- Cao SS, Kaufman RJ (2014) Endoplasmic reticulum stress and oxidative stress in cell fate decision and human disease. *Antioxid Redox Signal* 21:396–413
- Castegna A, Drake J, Pocemich C et al (2003) Protein carbonyl levels 161 161 protein carbonyl levels—an assessment of protein oxidation. In: Hensley K, Floyd RA (eds) *Methods in pharmacology and toxicology: Methods in biological oxidative stress*. © Humana Press Inc., Totowa
- Chakrabarti A, Chen AW, Varner JD (2011) A review of the mammalian unfolded protein response. *Biotechnol Bioeng* 108:2777–2793
- Close WH, Mount LE (1971) Energy retention in the pig at several environmental temperatures and levels of feeding. *Proc Nutr Soc* 30: 33A–34A
- Danial NN, Korsmeyer SJ (2004) Cell death: critical control points. *Cell* 116:205–219
- Davidson SM, Duchon MR (2006) Calcium microdomains and oxidative stress. *Cell Calcium* 40:561–574. <https://doi.org/10.1016/j.ceca.2006.08.017>
- Deldicque L (2013) Endoplasmic reticulum stress in human skeletal muscle: any contribution to sarcopenia? *Front Physiol* 4:236. <https://doi.org/10.3389/fphys.2013.00236>
- Dodd SL, Gagnon BJ, Senf SM, Hain BA, Judge AR (2010) Ros-mediated activation of NF-κB and foxo during muscle disuse. *Muscle Nerve* 41:110–113. <https://doi.org/10.1002/mus.21526>
- Dollberg S, Xi Y, Donnelly M M (1993) A noninvasive transcutaneous alternative to rectal thermometry for continuous measurement of core temperature in the piglet. *Pediatr Res* 34(4):512–517. <https://doi.org/10.1203/00006450-199310000-00026>
- Dupont-Versteegden EE (2006) Apoptosis in skeletal muscle and its relevance to atrophy. *World J Gastroenterol* 12:7463–7466. <https://doi.org/10.3748/wjg.v12.i46.7463>
- Ermak G, Davies KJA (2002) Calcium and oxidative stress: from cell signaling to cell death. *Mol Immunol* 38:713–721

- Frontera WR, Ochala J (2015) Skeletal muscle: a brief review of structure and function. *Calcif Tissue Int* 96:183–195. <https://doi.org/10.1007/s00223-014-9915-y>
- Fujii J, Homma T, Kobayashi S, Seo HG (2018) Mutual interaction between oxidative stress and endoplasmic reticulum stress in the pathogenesis of diseases specifically focusing on non-alcoholic fatty liver disease. *World J Biol Chem* 9:1–15. <https://doi.org/10.4331/wjbc.v9.i1.1>
- Gething MJ (1999) Role and regulation of the ER chaperone BiP. *Semin Cell Dev Biol* 10:465–472. <https://doi.org/10.1006/scdb.1999.0318>
- Gollnick PD, Sjödin B, Karlsson J et al (1974) Human soleus muscle: a comparison of fiber composition and enzyme activities with other leg muscles. *Pflugers Arch - Eur J Physiol* 348:247–255. <https://doi.org/10.1007/BF00587415>
- Harding HP, Zhang Y, Ron D (1999) Protein translation and folding are coupled by an endoplasmic-reticulum-resident kinase. *Nature* 397:271–274. <https://doi.org/10.1038/16729>
- Hildebrandt B, Wust P, Ahlers O et al (2002) The cellular and molecular basis of hyperthermia. *Crit Rev Oncol Hematol* 43:33–56
- Hissin PJ, Hilf R (1976) A fluorometric method for determination of oxidized and reduced glutathione in tissues. *Anal Biochem* 74(1):214–226. [https://doi.org/10.1016/0003-2697\(76\)90326-2](https://doi.org/10.1016/0003-2697(76)90326-2)
- Horimoto K, Nishimura Y, Oyama TM, Onoda K, Matsui H, Oyama TB, Kanemaru K, Masuda T, Oyama Y (2006) Reciprocal effects of glucose on the process of cell death induced by calcium ionophore or H₂O₂ in rat lymphocytes. *Toxicology* 225:97–108. <https://doi.org/10.1016/j.tox.2006.05.004>
- Iurlaro R, Muñoz-Pinedo C (2016) Cell death induced by endoplasmic reticulum stress. *FEBS J* 283:2640–2652
- Kaufman RJ (2002) Orchestrating the unfolded protein response in health and disease. *J Clin Invest* 110:1389–1398. <https://doi.org/10.1172/JCI16886>
- Kikusato M, Toyomizu M (2013) Crucial role of membrane potential in heat stress-induced overproduction of reactive oxygen species in avian skeletal muscle mitochondria. *PLoS One* 8:e64412. <https://doi.org/10.1371/journal.pone.0064412>
- Lara LJ, Rostagno MH (2013) Impact of heat stress on poultry production. *Animals* 3:356–369
- Lepock JR, Borrelli MJ (2005) How do cells respond to their thermal environment? *Int J Hyperthermia* 21(8):681–687. <https://doi.org/10.1080/02656730500307298>
- Levine RL, Garland D, Oliver CN et al (1990) Determination of carbonyl content in oxidatively modified proteins. *Methods Enzymol* 186:464–478. [https://doi.org/10.1016/0076-6879\(90\)86141-H](https://doi.org/10.1016/0076-6879(90)86141-H)
- Lima RB, Dos Santos TB, Vieira LGE et al (2013) Heat stress causes alterations in the cell-wall polymers and anatomy of coffee leaves (*Coffea arabica* L.). In: *Carbohydrate Polymers*. Elsevier 93(1):135–143. <https://doi.org/10.1016/j.carbpol.2012.05.015>
- Lin H, Jiao HC, Buyse J, Decuyper E (2006) Strategies for preventing heat stress in poultry. *Worlds Poult Sci J* 62:71–86. <https://doi.org/10.1079/wps200585>
- Lindquist S (1986) The heat-shock response. *Annu Rev Biochem* 55:1151–1191. <https://doi.org/10.1146/annurev.bi.55.070186.005443>
- Lindstedt SL (2016) Skeletal muscle tissue in movement and health: positives and negatives. *J Exp Biol* 219:183–188
- Lindstedt SL, Mineo PM, Schaeffer PJ, Schaeffer PJ (2013) Animal galloping and human hopping: an energetics and biomechanics laboratory exercise. *Adv Physiol Educ* 37:377–383. <https://doi.org/10.1152/advan.00045.2013.-This>
- Logue SE, Cleary P, Saveljeva S, Samali A (2013) New directions in ER stress-induced cell death. *Apoptosis* 18:537–546
- Loyau T, Bedrani L, Berri C, Métayer-Coustard S, Praud C, Coustham V, Mignon-Grasteau S, Duclos MJ, Tesseraud S, Rideau N, Hennequet-Antier C, Everaert N, Yahav S, Collin A (2014) Cyclic variations in incubation conditions induce adaptive responses to later heat exposure in chickens: a review. *Animal* 9:76–85. <https://doi.org/10.1017/S1751731114001931>
- Malhotra JD, Kaufman RJ (2007) Endoplasmic reticulum stress and oxidative stress: a vicious cycle or a double-edged sword? *Antioxid Redox Signal* 9:2277–2293
- Marklund S, Marklund G (1974) Involvement of the superoxide anion radical in the autoxidation of pyrogallol and a convenient assay for superoxide dismutase. *Eur J Biochem* 47:469–474. <https://doi.org/10.1111/j.1432-1033.1974.tb03714.x>
- Masuda K, Yamada T, Ishizawa R, Takakura H (2013) Role of myoglobin in regulating respiration during muscle contraction. *J Phys Fit Sport Med* 2(1):9–16. <https://doi.org/10.7600/jpfsm.2.9>
- McAnulty SR, McAnulty L, Pascoe DD et al (2005) Hyperthermia increases exercise-induced oxidative stress. *Int J Sports Med* 26:188–192. <https://doi.org/10.1055/s-2004-820990>
- McClung JM, Judge AR, Talbert EE, Powers SK (2009) Calpain-1 is required for hydrogen peroxide-induced myotube atrophy. *Am J Physiol - Cell Physiol* 296(2):C363–C371. <https://doi.org/10.1152/ajpcell.00497.2008>
- McClung JM, Judge AR, Powers SK, Yan Z (2010) p38 MAPK links oxidative stress to autophagy-related gene expression in cachectic muscle wasting. *Am J Physiol - Cell Physiol* 298(3):C542–C549. <https://doi.org/10.1152/ajpcell.00192.2009>
- Montilla SIR, Johnson TP, Pearce SC, Gardan-Salmon D, Gabler NK, Ross JW, Rhoads RP, Baumgard LH, Lonergan SM, Selsby JT (2014) Heat stress causes oxidative stress but not inflammatory signaling in porcine skeletal muscle. *Temperature* 1:42–50. <https://doi.org/10.4161/temp.28844>
- Moopanar TR, Allen DG (2006) The activity-induced reduction of myofibrillar Ca²⁺ sensitivity in mouse skeletal muscle is reversed by dithiothreitol. *J Physiol* 571:191–200. <https://doi.org/10.1113/jphysiol.2005.101105>
- Morishima N, Nakanishi K, Takenouchi H, Shibata T, Yasuhiko Y (2002) An endoplasmic reticulum stress-specific caspase cascade in apoptosis. Cytochrome c-independent activation of caspase-9 by caspase-12. *J Biol Chem* 277:34287–34294. <https://doi.org/10.1074/jbc.M204973200>
- Mujahid A, Yoshiki Y, Akiba Y, Toyomizu M (2005) Superoxide radical production in chicken skeletal muscle induced by acute heat stress. *Poult Sci* 84:307–314. <https://doi.org/10.1093/ps/84.2.307>
- Mujahid A, Sato K, Akiba YTM (2006) Acute heat stress stimulates mitochondrial superoxide production in broiler skeletal muscle, possibly via downregulation of uncoupling protein content. *Poult Sci* 85:1259–1265. <https://doi.org/10.1093/PS/85.7.1259>
- Mujahid A, Akiba Y, Warden CH, Toyomizu M (2007) Sequential changes in superoxide production, anion carriers and substrate oxidation in skeletal muscle mitochondria of heat-stressed chickens. *FEBS Lett* 581:3461–3467. <https://doi.org/10.1016/j.febslet.2007.06.051>
- Nakagawa T, Zhu H, Morishima N, Li E, Xu J, Yankner BA, Yuan J (2000) Caspase-12 mediates endoplasmic-reticulum-specific apoptosis and cytotoxicity by amyloid- β . *Nature* 403:98–103. <https://doi.org/10.1038/47513>
- Powers SK, Jackson MJ (2008) Exercise-induced oxidative stress: cellular mechanisms and impact on muscle force production. *Physiol Rev* 88:1243–1276
- Powers SK, Ji LL, Kavazis AN, Jackson MJ (2011) Reactive oxygen species: impact on skeletal muscle. *Compr Physiol* 1:941–969. <https://doi.org/10.1002/cphy.c100054>
- Renaudeau D, Collin A, Yahav S et al (2012) Adaptation to hot climate and strategies to alleviate heat stress in livestock production. *Animal* 6(5):707–728. <https://doi.org/10.1017/S1751731111002448>
- Richter K, Haslbeck M, Buchner J (2010) The heat shock response: life on the verge of death. *Mol Cell* 40:253–266
- Ron D, Walter P (2007) Signal integration in the endoplasmic reticulum unfolded protein response. *Nat Rev Mol Cell Biol* 8:519–529

- Roti Roti JL (2008) Cellular responses to hyperthermia (40–46 degrees C): cell killing and molecular events. *Int J Hyperther* 24:3–15
- Sahin K, Onderci M, Sahin N, Gursu MF, Kucuk O (2003) Dietary vitamin C and folic acid supplementation ameliorates the detrimental effects of heat stress in Japanese quail. *J Nutr* 133:1882–1886. <https://doi.org/10.1093/jn/133.6.1882>
- Shawka MN, Leon LR, Montain SJ, Sonna LA (2011) Integrated physiological mechanisms of exercise performance, adaptation, and maladaptation to heat stress. *Compr Physiol* 1:1883–1928. <https://doi.org/10.1002/cphy.c100082>
- Shenton D, Smirnova JB, Selley JN, Carroll K, Hubbard SJ, Pavitt GD, Ashe MP, Grant CM (2006) Global translational responses to oxidative stress impact upon multiple levels of protein synthesis. *J Biol Chem* 281:29011–29021. <https://doi.org/10.1074/jbc.M601545200>
- Smuder AJ, Hudson MB, Nelson WB, Kavazis AN, Powers SK (2012) Nuclear factor- κ B signaling contributes to mechanical ventilation-induced diaphragm weakness*. *Crit Care Med* 40:927–934. <https://doi.org/10.1097/CCM.0b013e3182374a84>
- Sonna LA, Fujita J, Gaffin SL, Lilly CM (2002) Invited review: effects of heat and cold stress on mammalian gene expression. *J Appl Physiol* 92:1725–1742
- St-Pierre NR, Cobanov B, Schnitkey G (2003) Economic losses from heat stress by US livestock industries. *J Dairy Sci* 86:E52–E77. [https://doi.org/10.3168/jds.S0022-0302\(03\)74040-5](https://doi.org/10.3168/jds.S0022-0302(03)74040-5)
- Swanlund JM, Kregel KC, Oberley TD (2008) Autophagy following heat stress: the role of aging and protein nitration. *Autophagy* 4:936–939. <https://doi.org/10.4161/auto.6768>
- Syafwan S, Kwakkel RP, Verstegen MWA (2011) Heat stress and feeding strategies in meat-type chickens. *Worlds Poult Sci J* 67:653–674
- Tattersson AJ, Hahn AG, Martini DT, Febbraio MA (2000) Endoplasmic reticulum. *J Sci Med Sport* 3:186–193. [https://doi.org/10.1016/S1440-2440\(00\)80080-8](https://doi.org/10.1016/S1440-2440(00)80080-8)
- Trachootham D, Lu W, Ogasawara MA, Valle NRD, Huang P (2008) Redox regulation of cell survival. *Antioxid Redox Signal* 10:1343–1374
- Verstegen MWA, Close WH, Start IB, Mount LE (1973) The effects of environmental temperature and plane of nutrition on heat loss, energy retention and deposition of protein and fat in groups of growing pigs. *Br J Nutr* 30:21–35. <https://doi.org/10.1079/bjn19730005>
- Wang M, Kaufman RJ (2016) Protein misfolding in the endoplasmic reticulum as a conduit to human disease. *Nature* 529:326–335
- Wang Y-X, Zhang C-L, Yu RT, Cho HK, Nelson MC, Bayuga-Ocampo CR, Ham J, Kang H, Evans RM (2004) Regulation of muscle fiber type and running endurance by PPAR δ . *PLoS Biol* 2:e294. <https://doi.org/10.1371/journal.pbio.0020294>
- Whidden MA, Smuder AJ, Wu M, Hudson MB, Nelson WB, Powers SK (2010) Oxidative stress is required for mechanical ventilation-induced protease activation in the diaphragm. *J Appl Physiol* 108:1376–1382. <https://doi.org/10.1152/jappphysiol.00098.2010>
- Witko-Sarsat V, Friedlander M, Capeillère-Blandin C et al (1996) Advanced oxidation protein products as a novel marker of oxidative stress in uremia. *Kidney Int* 49(5):1304–1313. <https://doi.org/10.1038/ki.1996.186>
- Wu J, Kaufman RJ (2006) From acute ER stress to physiological roles of the unfolded protein response. *Cell Death Differ* 13:374–384
- Xu C, Bailly-Maitre B, Reed JC (2005) Endoplasmic reticulum stress: cell life and death decisions. *J Clin Invest* 115:2656–2664
- Yahav S (2009) Alleviating heat stress in domestic fowl: different strategies. *Worlds Poult Sci J* 65:719–732
- Zhang K, Kaufman RJ (2008) Identification and characterization of endoplasmic reticulum stress-induced apoptosis in vivo. *Methods Enzymol* 442:395–419
- Zhang L, Kimball SR, Jefferson LS, Shenberger JS (2009) Hydrogen peroxide impairs insulin-stimulated assembly of mTORC1. *Free Radic Biol Med* 46:1500–1509. <https://doi.org/10.1016/j.freeradbiomed.2009.03.001>
- Zhang ZY, Jia GQ, Zuo JJ, Zhang Y, Lei J, Ren L, Feng DY (2012) Effects of constant and cyclic heat stress on muscle metabolism and meat quality of broiler breast fillet and thigh meat. *Poult Sci* 91:2931–2937. <https://doi.org/10.3382/ps.2012-02255>
- Zima AV, Blatter LA (2006) Redox regulation of cardiac calcium channels and transporters. *Cardiovasc Res* 71:310–321

Publisher's note Springer Nature remains neutral with regard to jurisdictional claims in published maps and institutional affiliations.